Computer Simulation of the Phosphorylation Cascade Controlling Bacterial Chemotaxis

Dennis Bray,* Robert B. Bourret,†‡ and Melvin I. Simon†

*Department of Zoology, University of Cambridge, Cambridge CB2 3EJ, United Kingdom; and
†Division of Biology, California Institute of Technology, Pasadena, California 91125

We have developed a computer program that simulates the intracellular reactions mediating the rapid (nonadaptive) chemotactic response of *Escherichia coli* bacteria to the attractant aspartate and the repellent Ni^{2+} ions. The model is built from modular units representing the molecular components involved, which are each assigned a known value of intracellular concentration and enzymatic rate constant wherever possible. The components are linked into a network of coupled biochemical reactions based on a compilation of widely accepted mechanisms but incorporating several novel features. The computer motor shows the same pattern of runs, tumbles and pauses seen in actual bacteria and responds in the same way as living bacteria to sudden changes in concentration of aspartate or Ni^{2+}. The simulated network accurately reproduces the phenotype of more than 30 mutants in which components of the chemotactic pathway are deleted and/or expressed in excess amounts and shows a rapidity of response to a step change in aspartate concentration similar to living bacteria. Discrepancies between the simulation and real bacteria in the phenotype of certain mutants and in the gain of the chemotactic response to aspartate suggest the existence of additional as yet unidentified interactions in the *in vivo* signal processing pathway.

INTRODUCTION

Coupled protein phosphorylations are a universal mechanism of intracellular signaling and the basis of many complex nets of reactions in eucaryotic cells. Such networks are poorly understood, despite their importance, because of the large number of components involved, and the multiple links that exist between them. Not only are quantitative data on the individual reactions lacking, but we also lack a vehicle by which we can comprehend the implications of such data and verify the overall performance of the entire network. Without making many detailed calculations, it will be difficult to predict how the network performs under a particular set of starting conditions, whether it will ever show oscillatory or chaotic behavior, and how the performance of the network will be affected by genetic modifications.

The rational solution to this problem is to employ a computer simulation that can be used to catalogue biochemical data, test current hypotheses of mechanism, and make predictions of performance under a virtually

‡ Present address: Department of Microbiology and Immunology, University of North Carolina, Chapel Hill, NC 27599.

limitless variety of conditions. However, there have been very few attempts to develop quantitative models of this sort for cell signaling pathways involving coupled phosphorylation reactions. Early steps in this direction include models of the spatial propagation of oscillations in Ca^{2+} concentration in a variety of cells (reviewed by Dupont and Goldbeter, 1992) and the initial response to light of vertebrate photoreceptors (Lamb and Pugh, 1992). For the vast majority of cell signaling pathways, there is insufficient information to construct a meaningful simulation. Without knowing most of the relevant intracellular concentrations and enzymatic rate constants in a pathway, computer simulations can only be phenomenological representations having little analytical power or predictive force at the molecular level.

One of the few signaling pathways for which there is presently sufficient information to attempt a detailed computer simulation is that underlying the chemotactic response in coliform bacteria. This entails a small and defined set of intracellular proteins which, through coupled phosphorylation and methylation reactions, enable the bacterium to respond in an informed, if not intelligent, way to its chemical environment. All of the intracellular proteins involved in this response have

been sequenced and purified. Many of the enzymatic reactions they catalyze have been analyzed kinetically. Mutants lacking identified proteins either singly or in combination have been isolated in large numbers and their chemotactic responses documented. There is, in short, a uniquely large and complete set of data, unmatched in any other cell signaling system, against which a model can be tested.

We have therefore undertaken to simulate the biochemical reactions of bacterial chemotaxis in a computer program, which we hope will eventually reproduce all the salient biochemical, genetic and behavioral observations made on living bacteria. As the first step toward this aim we describe in this paper the simulation of the chain of signals from the cell surface receptor to the flagellar motor that mediate the rapid, excitatory response to specific attractants and repellents. The slower adaptation of the system due to receptor methylation, the kinetics of which have been modeled previously (Goldbeter and Koshland, 1982; Asakura and Honda, 1984), is not part of the present model.

MATERIALS AND METHODS

Signal Pathway

To provide a background to the model described in this paper, we now review briefly the protein reactions that carry the chemotactic signal from the membrane receptor to the flagellar motor.

The chemotactic response of coliform bacteria such as *Escherichia coli* and *Salmonella typhimurium* depends on the ability to modulate swimming behavior in response to external stimuli. This is achieved with linked chains of protein phosphorylation, which carry signals from the membrane receptors to the flagellar motor (Figure 1) (Bourret et al., 1991; Stock et al., 1991, 1992). Although many details are still debated, it is widely accepted that binding of an attractant or repellent molecule to a receptor changes the rate of autophosphorylation of an intracellular protein kinase, denoted CheA[1] (Borkovich et al., 1989; Borkovich and Simon, 1990; Ninfa et al., 1991). The phosphorylated form of CheA (CheAp) transfers its phosphate group to a second protein CheY (Hess et al., 1988c; Wylie et al., 1988). The product of this phosphotransferase reaction, CheYp, interacts with the flagellar motor so as to increase clockwise rotation, which produces "tumble" swimming behavior. The default state of the motor in the absence of CheYp is counterclockwise rotation, which results in "run" swimming behavior (Larsen et al., 1974; Parkinson, 1978). Two other components involved in this direct or "excitation" response are CheW, which appears to mediate the effect of receptor on CheA phosphorylation (Borkovich et al., 1989; Borkovich and Simon, 1990; Ninfa et al., 1991) and CheZ, which counteracts the effect of CheYp by dephosphorylation (Hess et al., 1988a,c). Flagellar rotation is also modified on a slower time scale by the methylation of receptor proteins by a methyltransferase CheR (Springer and Koshland, 1977), and by the removal of these methyl groups by the methylesterase CheB (Stock and Koshland, 1978). Like CheY, the methylesterase CheB is regulated by phosphotransfer from CheAp (Hess et al., 1988c; Lupas and Stock, 1989; Stewart et al., 1990).

Our model concerns the chain of coupled protein phosphorylations that carry signals from the Tar receptor to the flagella motor, not the modification of the Tar receptor by methylation, which forms the
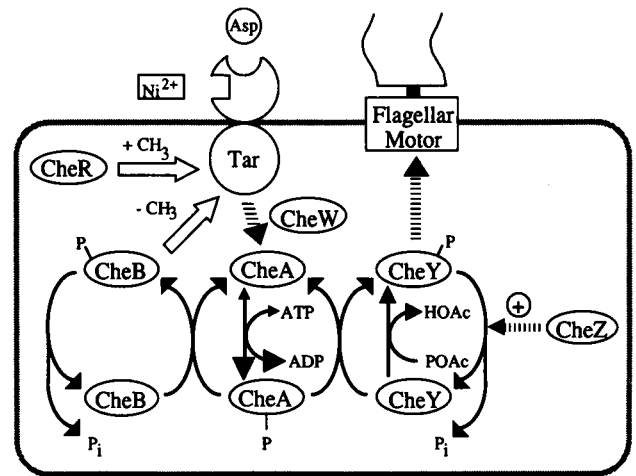
[1] Abbreviations used: A, CheA; asp, aspartate; B, CheB; M, flagellar motor; ni, Ni^{2+} ion; p, phosphorylated form of indicated protein; R, CheR; T, Tar; W, CheW; Y, CheY; Z, CheZ.

Figure 1. Signal transduction pathway in bacterial chemotaxis. Symbols within circles denote the Che proteins, in some cases phosphorylated, which carry the chemotactic signals from the receptor protein Tar to the flagellar motor. Solid arrows represent phosphorylation reactions. Dashed arrows indicate regulatory interactions. The methylation reactions catalyzed by CheR and CheB (open arrows) are not included in the computer simulation.

basis of the adaptation of this response. In consequence, we do not expect the model to show the slow recovery of swimming behavior characteristic of wild-type bacteria, but it should be able to reproduce the short-term, impulsive responses of wild-type and mutant bacteria. It should also reflect the short-term behavior of mutants in which the demethylating enzyme CheB has been removed or overexpressed, because the latter protein forms part of the flux of phosphate groups in the excitatory pathway.

Theory

In this section we present the algorithms used to represent the signaling reactions and the assumptions inherent in their use.

Information on the binding of aspartate or Ni^{2+} to the Tar receptor is relayed through the cytoplasm by changes in the concentrations of various phosphorylated protein species. It is convenient to divide the individual steps in this cascade into *binding steps*, in which two molecular components associate or disassociate, and *reaction steps* in which a phosphate group is added or removed from a protein. Each step is represented by an equation which is evaluated repeatedly at intervals of time Δt, which is typically 5 ms.

Experimentally, the response of bacteria to a step change in attractant or repellant concentration occurs in $\sim$0.2 s (Segall et al., 1982) and evidence of a delay due to diffusion has been obtained only in abnormally long filamentous mutants (Segall et al., 1985). No data is available regarding on and off rates for individual binding reactions. Given the observed rapidity of signal propagation through the entire pathway, and for the sake of computational stability, we therefore make the simplest assumption, namely that individual binding steps reach equilibrium within each iteration cycle. Note that the concentrations of binding species will nevertheless change with time due to the phosphorylation and dephosphorylation reactions described below.

Binding of a small molecular weight ligand L that is in large excess to a protein receptor R, specifically the binding of aspartate or Ni^{2+} to Tar in one of its complexed forms, is described by the simple binding equation

$$[RL] = [Ro]\left\{\frac{[Lo]}{[Lo] + Kd}\right\}$$

470

where [Ro] and [Lo] are the total concentrations of receptor and ligand, respectively, [RL] is the concentration of the protein-ligand complex, and Kd is the dissociation constant of the complex.

All other binding steps in the simulation involve the association of cytoplasmic proteins at comparable, and usually low, concentrations and for this we use the relationship:

$$[RL] = 0.5\{[Ro] + [Lo] + Kd - \sqrt{([Ro] + [Lo] + Kd)^2 - 4[Ro] \times [Lo]}\}$$

where [Ro] and [Lo] are arbitrarily assigned to the two proteins (see Segel, 1975).

Reaction steps are not assumed to run to completion within Δt and are integrated by successive steps of the simulation. For protein autophosphorylations we use the simple Michaelis-Menten relationship

$$v = [E]\left\{\frac{k\_cat \times [ATP]}{[ATP] + Km}\right\}$$

where v is the rate of formation of the phosphorylated species in moles per second, [E] is the free enzyme concentration, [ATP] is the concentration of ATP, k_cat is the catalytic rate constant and K_m is the Michaelis constant (Michaelis and Menten, 1913; Fersht, 1984). For all other reactions we assume that the concentrations of reacting species are small, so that the reactions are simply described by

$$v = (k\_cat/Km) [E] \times [S]$$

or, for autodephosphorylations

$$v = k\_cat [E]$$

Flagellar Motor

Unlike all other components of the simulation, the flagellar motor is not a single molecular species. It is a complex structure, built from approximately 40 distinct proteins that rotates either clockwise or counterclockwise at speeds of ≤300 cycles/s (significantly less when the bacterium is tethered to a surface) (Jones and Aizawa, 1991). The direction of rotation is controlled by the phosphorylated form of CheY through an interaction with the switch components (FliG, FliM, and FliN proteins) of the motor (Jones and Aizawa, 1991). The interaction appears to be a simple binding of CheYp rather than a phosphotransfer reaction (Bourret et al., 1990).

It was shown previously by Block et al. (1982, 1983) that a simple two-state model in which run and tumble states differ in the binding of a single ligand has similar stochastic properties to the runs and

Different states of the flagellar motor (M) are determined by the binding of CheYp (Yp):

State '1'	M	ccw rotation	(run)
State '3'	MYp	ccw rotation	(run)
State '5'	MYpYp	zero rotation	(pause)
State '7'	MYpYpYp	cw rotation	(tumble)
State '9'	MYpYpYpYp	cw rotation	(tumble)

Occupation of the different states is governed by reversible equilibria:

M + Yp ⇌ MYp	$K_1 = k_{1l}/k_{1r}$
MYp + Yp ⇌ MYpYp	$K_2 = k_{2l}/k_{2r}$
MYpYp + Yp ⇌ MYpYpYp	$K_3 = k_{3l}/k_{3r}$
MYpYpYp + Yp ⇌ MYpYpYpYp	$K_4 = k_{4l}/k_{4r}$

Apparent dissociation constants for the different states are determined by two constants, α and κ:

$$K_1 = \kappa/4 \quad K_2 = 2\alpha\kappa/3 \quad K_3 = 3\alpha^2\kappa/2 \quad K_4 = 4\alpha^3\kappa$$

Figure 2. Multiple equilibria between the flagellar motor complex (M) and the phosphorylated form of CheY (Yp) used to calculate motor behavior.
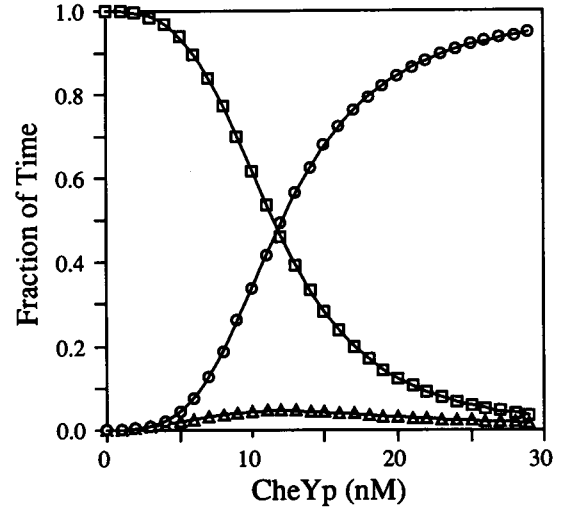

Figure 3. Proportion of time spent in run (□), tumble (O), and pause (△) modes predicted for the flagellar motor model, with the resting concentration of CheYp in a wild-type bacterium set to 9 nM.

tumbles of the flagellar motor. In the present simulation, this model has been extended to incorporate two additional features. One is the cooperativity between CheY levels and flagellar motor response seen in mutant strains in which CheY is over-expressed to different levels (Kuo and Koshland, 1989). The effective species is now thought to be CheYp. The other feature added to the motor model is the capacity for pausing, which has been reported by Eisenbach and colleagues to be an inherent part of the behavioral repertoire of coliform bacteria (Lapidus et al., 1988; Eisenbach et al., 1990).

These observations are incorporated into a model in which the motor complex, denoted M, binds sequentially up to four CheYp molecules thereby producing five distinct molecular species. Two of these (M and MYp) rotate counterclockwise, another two (MYpYpYp and MYpYpYpYp) rotate clockwise, and one species (MYpYp) is stationary, corresponding to the pausing of the motor (Figure 2). In a population of bacteria, the rotational bias (defined as the fraction of time spent in the counterclockwise mode) is therefore given by the following:

$$bias = \frac{M + MYp}{M + MYp + MYpYp + MYpYpYp + MYpYpYpYp}$$

As in the earlier model of Block et al. (1982, 1983), transitions between each pair of states are governed by paired first-order rate constants, such as k_{1r} and $k_{2r}Yp$ (which is pseudo first-order at a given concentration of Yp). For an individual motor, these rate constants represent the probabilities per unit time of terminating the current state.

The Adair-Pauling model of a multisite allosteric enzyme allows dissociation constants for each binding step to be calculated from two parameters—the dissociation constant of binding of the first binding site (κ) and the factor (α) by which the affinity of successive binding sites change (Segel, 1975). We have assumed that the flagellar motor is similarly well-behaved and calculated κ and α from an arbitrarily assigned value for the resting (unstimulated) concentration of CheYp and from the observed proportion of time spent in runs, pauses, and tumbles of an unstimulated, wild-type bacterium (Lapidus et al., 1988; Eisenbach et al., 1990). In trial simulations we found that the resting concentration of CheYp could be varied over a wide range without affecting overall performance. In the absence of experimental data bearing on this value, we selected 9 nM, which in combination with the best available values of reaction rates, produces an approximately wild-type rotational bias for mutant strains lacking either Tar, CheW, and CheZ; Tar and CheZ; or CheW and CheZ (Liu and Parkinson,
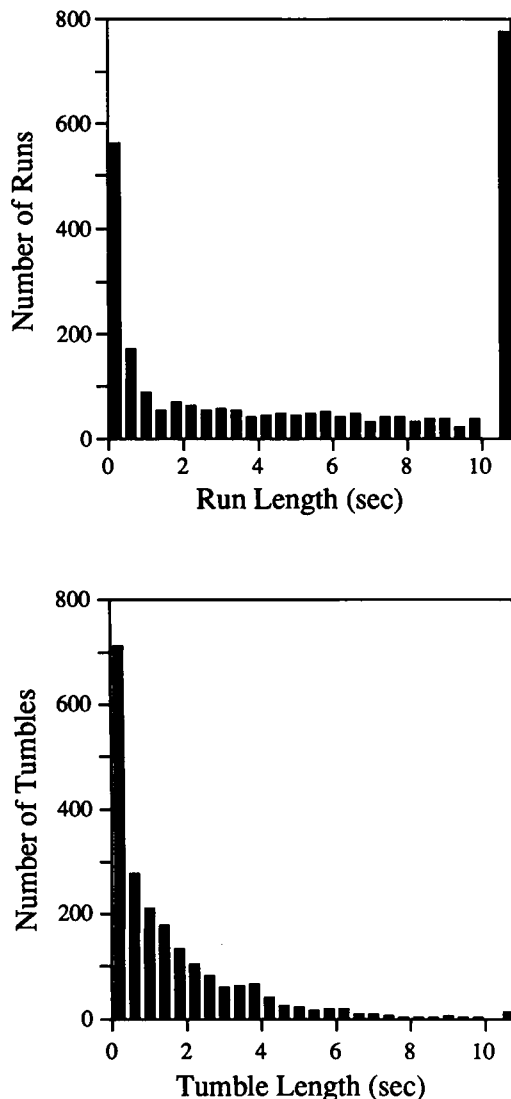
Figure 4. Durations of runs and tumbles predicted for a wild-type unstimulated bacterium using a random number generator. The last category in each histogram represents all episodes > 10 s in length. Results from 5×10^6 simulation cycles are displayed, totaling 2595 runs and 2093 tumbles. There were also 4683 pauses during the same period distributed as follows: 0–0.4 s, 4250; 0.4–0.8 s, 403; 0.8–1.2 s, 29; 1.2–1.6 s, 1; >1.6 s, 0. The run and tumble distributions conform closely to experimentally determined values (see Block *et al.*, 1983).

1989). This choice results in values of $\alpha = 0.14$, and $\kappa = 2.25 \times 10^{-7}$ M. Figure 3 shows the changes in proportion of time spent in runs, tumbles, and pauses as CheYp changes in concentration. The distribution corresponds to positive cooperativity between CheYp and the rotational bias with a Hill coefficient of about 3.0.

The multiple equilibria shown in Figure 2, which represent the steady state population levels of the different rotational forms, can also be used to reproduce the stochastic behavior of a single motor, as might be observed in a bacterium tethered to a coverslip with a single flagellar hook (Silverman and Simon, 1974). A similar calculation, although simpler, was made by Block *et al.* (1982) in respect to their 2-state model. Thus with reference to Figure 2, the probability that a given motor currently in state "3" will change to state "5" in

the next time interval of dt s, is k_{2r}Ypdt. The probability that a motor that is currently turning counterclockwise (that is, in *either* state "1" *or* state "3") will stop (move to state "5") in the next time interval is given by

$$k_{2r}[\text{Yp}]dt\left(\frac{[\text{MYp}]}{[\text{M}] + [\text{MYp}]}\right)$$

Similar expressions exist for the termination of tumbles and pauses. Values of the rate constants k_{2r}, k_{3l}, k_{3r}, and so on were estimated from the dissociation constants of individual reactions ($K_1 = k_{1r}/k_{1l}$ etc.) in conjunction with the experimentally observed proportions of runs, tumbles, and pauses seen in unstimulated wild-type bacteria. Probabilities of transition between the different states of the motor model were derived from these rate constants. Then the history of an individual flagellar motor was simulated by starting it in state 1 (see Figure 2) and allowing a random number generated within the program to determine, at each cycle, whether the motor changed in state 3. If and when the motor arrived at state 3, then a similar procedure determined whether, in successive cycles, it changed to state 5 or back to state 1. In this way the stochastic behavior of a single flagellar motor was stimulated. The performance of wild-type, unstimulated motors modeled according to this prescription, is closely similar to that described experimentally, as illustrated in Figure 4 (see also Figure 6).

Numerical Integration

The simulation uses a procedure in which each binding or reaction step is taken in turn and the concentrations of the reactants and products are updated according to the appropriate algorithm. Changes within a reaction step are predicted by the Euler method. We selected this rudimentary integration procedure rather than one of the many more sophisticated routines available because it makes it easy to treat individual reactions separately for display purposes and because of the computational stability it provides. Because each reaction or binding step is taken in turn there is no possibility of extrapolated concentrations exceeding the available material. The program is thus extremely robust, and ligand concentrations from 10^{-12} to 1M can be applied without causing instability. Similarly, levels of enzymes can be manipulated by "mutation" ad libitum.

The primary disadvantage of the method we have selected is its inaccuracy when compared with the more usual methods of numerical integration. As already mentioned, however, the values of binding constants and rate constants available to us are only crude approximations to the actual kinetic parameters within the cell. Our primary purpose here is to summarize the existing body of research in a simple formulation and to test whether it gives approximately the correct response following a variety of mutational modifications, and for this the procedure we have used is adequate.

As with any form of numerical integration, there is the opportunity to increase accuracy by reducing the step-size. Tests of the present simulation with wild-type bacteria over a range of repellent and attractant concentrations, showed stable values of rotational bias, with <1% variation for step sizes in the range 10^{-4} to 10^{-2} s.

Data Management

The program was written in "C" on a Macintosh IIfx microcomputer using a Think C compiler (Symantec Corporation, Cupertino, CA). A PC-compatible version was prepared by Alastair Brown (MRC Human Genetics Project, Edinburgh, Scotland) using a Microsoft C compiler (Microsoft, Version 6.0) and run on an Elonex PC 433. The core of the program is a series of 21 functions each of which represents a single step in the signaling cascade. The entire series is performed in sequence, once for each cycle of the simulation, the number of cycles, and the bacterial time represented by each cycle both being set by the user. All simulations reported in this manuscript used a cycle representing 5 ms of elapsed time. A typical run might entail 2000

cycles and occupy 1–2 s of real time on either the Macintosh or the Elonex.

Data used by the program are contained in four files, each of which can be modified by the user. These include specifications of the intracellular concentration of ATP, the time duration and number of cycles, the resting concentration of CheYp in a wild-type bacterium; a listing of primary gene products used in the program, together with the number of molecules per cell; a listing of all the molecular species whose activity or concentration changes during the simulation; and the rate constants and other information relating to the reactions (both binding interactions and enzyme catalyzed steps) in the simulation. Other parameters, such as the genotype of the organism, the stimulus applied to it, and the starting phenotype can be specified by the user while the program is running. Concentrations of the signaling molecules are stored at the beginning and end of the simulation, and at specified intervals in between, and can be retrieved for analysis and display. An error-detection algorithm monitors the stoichiometry of each of eight protein species and indicates if any have changed by more than a predetermined amount during the simulation.

The program allows signaling molecule concentrations to be displayed either all of them at a given time, or selected signals throughout the simulation. It also allows the behavior of individual bacterial motors to be simulated (as opposed to the average performance of large numbers of bacteria) by applying a Monte Carlo randomization procedure to the coupled equilibria representing the flagellar motor. Two other quantities are calculated during the simulation and can be displayed on completion of a simulation. One is the rotational bias (the proportion of time a flagellar motor spends in ccw rotation) which is calculated with each cycle of the simulation. The second is the chemotactic gain, here defined as the change in rotational bias caused by a 1% change in receptor occupancy by aspartate. The gain is calculated at the end of each simulation by increasing the concentration of aspartate by 1 nM, performing an additional 1 second run, and then normalizing the resulting change in bias to the change in receptor occupancy.

An important feature of the program is the provision of internal test routines that allow simulations to be run autonomously. Routines available to the user include a test in which the concentration of a Che protein, selected by the user, is incremented, a rate test in which a selected rate constant is incremented, and a test in which the chemotactic behavior of a selected set of mutant bacteria is calculated and displayed. Tests of this kind were essential in the development of the program, as described below.

Tethering Experiments

To further evaluate the model, we examined the behavior of several bacterial strains for which no published data were available. RP437recA is wild type for chemotaxis (Bourret et al., 1990); its complete genotype is thr(am)1 leuB6 his4 metF(am)159 eda50 rpsL136 thi1 ara14 lacY1 mtl1 xyl5 tonA31 tsx78 recAΔ(SstII-EcoRI) srl::Tn10. KO642recA was made by P1 transduction of recAΔ(SstII-EcoRI) srl::Tn10 into RP1616, which carries cheZΔ6725 (Liu and Parkinson, 1989). The complete genotype of KO642recA is cheZΔ6725 thr(am)1 leuB6 his4 metF(am)159 rpsL136 thi1 ara14 lacY1 mtl1 xyl5 tonA31 tsx78 recAΔ(SstII-EcoRI) srl::Tn10. Plasmids pRBB28 (p_{trp} cheA ori$_{pBR322}$Amp^R) (Bourret et al., 1993), pRBB30 (p_{trp} cheAW ori$_{pBR322}$ Amp^R) (Bourret et al., 1993), pRBB40 (p_{trp} cheYZ ori$_{pBR322}$ Amp^R) (Bourret et al., 1990), and pKB24 (p_{tac} cheB ori$_{pACYC184}$ Cam^R) (Borkovich et al., 1992) have been described. pRBB43 (p_{trp} cheA ori$_{pBR322}$ Amp^R) was made by deleting the "cheW tar" EcoRV-PvuII fragment from pRBB28. The following strains were evaluated (see Table 5) A^{2+}W^{2+} = RP437recA/pRBB30, Y^{2+}Z^{2+} = RP437recA/pRBB40, A^{2+}Z$^-$ = KO642recA/pRBB43, and B^{2+}Z$^-$ = KO642recA/pKB24.

Bacterial cultures for tethering experiments were grown overnight in T broth (1% tryptone, 0.5% NaCl) with appropriate antibiotics, at 30°C. Cultures were diluted 50-fold into fresh media, coded to reduce observer bias, and grown 2 h at 30°C. Appropriate inducer [100 μg/ml β-indoleacrylic acid or 1 mM isopropylthiogalactose (IPTG)] was

then added and incubation continued until the culture reached OD$_{600}$ ≈ 0.4 (another 2 h). The cells were collected by centrifugation and resuspended in an equal volume of ice-cold KEP-buffer (10 mM potassium phosphate, pH 7.0, 0.1 mM EDTA). Flagella were sheared off by 15-s treatment with a Brinkmann Homogenizer (Westbury, NY, Model PT 10/35). Bacteria were collected by brief centrifugation to remove free flagella, resuspended in an equal volume of ice cold KEP, and centrifuged again. The cell pellets were left on ice until use and then resuspended in an equal volume of ice cold tethering buffer (KEP + 10 mM sodium lactate, 75 mM NaCl, 0.1 mM L-methionine, and 100 μg/ml chloramphenicol). An aliquot of bacteria was mixed with an appropriate dilution of anti-flagellar antibody, placed on a coverslip, and allowed to adhere ≥10 min at room temperature. The coverslip was then rinsed with tethering buffer, inverted over a chamber containing tethering buffer, and ≥20 rotating cells observed ≥20 s each.

RESULTS

Development of the simulation entailed selection of a suitable biochemical network of intracellular reactions, the choice of algorithms to represent these reactions, and the allocation of intracellular concentrations and rate constants. Experimental data on many of the required intracellular concentrations and rate constants are lacking (and there are still doubts about certain aspects of the reaction pathway) so that any model at this stage has to be to some extent hypothetical. Many of the parameters used in the program are averaged, or are consensus values taken from various primary sources. Published values for the periods of time spent in runs and tumbles of wild type unstimulated E. coli, for example, correspond to biases from 0.64 to 0.86 (Berg and Brown, 1972; Block et al., 1982), and we have assumed it to be 0.70. Similar compromises were also made in assigning concentrations of Che proteins (Table 1) and enzymatic rate constants (Table 2).

To assign values to rate constants and concentrations for which no experimental information is available, a "boot-strapping" strategy was adopted in which Che proteins were added one by one to a mutant strain lacking everything but the flagellar motor (a "gutted" strain). As each signaling protein was included, intracellular concentrations and reaction rates were assigned from published literature if possible. Parameters for which no experimental data existed were titrated, using the internal test routines, until the chemotactic performance of the simulation matched the performance of actual bacteria with a corresponding genotype.

Phosphate Flux

The intracellular concentration of CheYp, the determinant of motor rotation, is maintained by the series of linked cyclic phosphorylations and dephosphorylations shown in Figure 1. The cycle is driven by the kinase CheA, which catalyzes the transfer of phosphate groups from ATP to its own histidine residue (Hess et al., 1988b). Phosphorylated CheA then transfers its phosphate group to CheY or CheB (the demethylating enzyme, here included solely for its participation in the

Table 1. Amounts of chemotaxis proteins used in the *bct 1.1* simulation

Protein	Molecules/ cell	Concentration (μM)[a]	References[b]
Tar	4 250	5	Clarke and Koshland (1979); Hazelbauer and Engstrom (1981); Ninfa *et al.* (1991); Gegner *et al.* (1992)
CheR	850	1	DeFranco and Koshland (1981); Stock *et al.* (1991)
CheB	1 700	2	DeFranco and Koshland (1981); Stock *et al.* (1991)
CheW	4 250	5	Ninfa *et al.* (1991); Gegner *et al.* (1992); Matsumura *et al.* (1990); Gegner and Dahlquist (1991)
CheA	4 250	5	Ninfa *et al.* (1991); Gegner *et al.* (1992); Matsumura *et al.* (1990); Gegner and Dahlquist (1991)
CheY	8 500	10	Stock *et al.* (1985); Kuo and Koshland (1987)
CheZ	17 000	20	Matsumura *et al.* (1990); Kuo and Koshland (1987)
Motor	8.5	0.01	Jones and Aizawa (1991)

[a] Concentration is calculated based on a cell volume of 1.41×10^{-15} L (Kuo and Koshland, 1987).

[b] Numbers of molecules are rounded-off, consensus values, based on the references.

flow of phosphate groups) (Hess *et al.*, 1988c; Wylie *et al.*, 1988). CheY can also autophosphorylate by using acetyl phosphate as a phosphate donor (Lukat *et al.*, 1992). CheYp and CheBp both spontaneously autodephosphorylate; in addition, CheZ mediates a more rapid loss of phosphate groups from CheYp (Hess *et al.*, 1988a,c; Wylie *et al.*, 1988). The principal reactions in this cascade are shown schematically in Figure 5.

Each branch point in the network of Figure 5 will be subject to conservation laws analogous to the Kirchoff Laws for the flow of electrical current in a circuit. For example, the rate of formation of CheYp by phospho-transfer from CheAp to CheY and by autophosphorylation with acetyl phosphate must balance the loss of CheYp by autodephosphorylation and by the action of CheZ. Constraints of this kind permit the estimation of individual reaction rates that have not been determined experimentally.

Data used to solve the network shown in Figure 5 are given in Tables 1 and 2 together with the results of predicting values by the procedure just mentioned. The latter include values for the total intracellular concentration of each of the signaling proteins (no experimental evidence is presently available on the concentrations of phosphorylated species) and for three kinetic rates that have not so far been measured.

Tar, CheW, and CheA

In order for the phosphorylation system to respond to externally applied attractants and repellents there must be a kinetic link between Tar and CheA. Mutant analysis indicates that both CheW and Tar are needed for the response to attractants (Wolfe *et al.*, 1987; Conley *et al.*, 1989) and experiments with purified components indicate that Tar in conjunction with CheW markedly increases the rate of CheA autophosphorylation (Borkovich and Simon, 1990; Ninfa *et al.*, 1991). Experiments have also been performed in which CheW and Tar are overproduced, leading to the paradoxical observation that the absence of one of these proteins gives the same phenotype (persistent smooth swimming) as does its overexpression (Stewart *et al.*, 1988; Liu and Parkinson, 1989; Sanders *et al.*, 1989). Recent studies indicate the formation of a ternary complex containing Tar, CheW, and CheA that is capable of increasing the rate of CheA autophosphorylation (Gegner *et al.*, 1992).

The precise mechanism(s) by which Tar, CheW, and CheA interact in vivo is uncertain at present. For simplicity we have adopted the symmetrical set of binding interactions listed in Table 3, which includes two reactions (binding of Tar and CheA and of CheW to the complex of Tar and CheA) for which there is presently no experimental evidence and predictions for three as yet undetermined reaction rates. The ternary complex of Tar, CheW, and CheA (TWA) is then postulated to stimulate CheA phosphorylation catalytically, thereby introducing a tumble signal. The influence of aspartate on the system is introduced by assuming that aspartate binds to Tar with the same affinity regardless of its association with CheW and CheA and that the aspartate-containing TWA complex, (Tasp-WA) is inactive in increasing CheA autophosphorylation. The repellent properties of Ni^{2+} are accounted for by assuming that the nickel-containing TWA complex (Tni-WA) stimulates CheA autophosphorylation at an even higher rate than TWA alone.

Gain and Response Time

Completion of the chain of signals from receptor Tar to the flagellar motor enables the response of the complete system to changes in attractant or repellent to be examined. Because an adaptation component is presently lacking in the model, we do not expect it to show the slow recovery of swimming behavior characteristic of wild-type bacteria. The model should however be able to reproduce the short-term, impulsive response of wild-type bacteria. The contents of a file listing amounts of all the signaling molecules in a sample simulation is shown in Table 4.

Changes in performance of a single motor, displayed as a time course of runs, pauses, and tumbles before and after addition of 1 μM aspartate are shown in Figure 6. The pattern of rotation in this figure is closely similar

Table 2. Rates of phosphorylation reactions used in the *bct 1.1* simulation

Reaction	Rate constant[a]	Source
Autophosphorylation of CheA by ATP A → Ap	1×10^{-3} s^{-1} [b,c]	Borkovich and Simon (1990)
TWA-stimulated autophosphorylation of CheA TWA + A → TWA + Ap	5.9×10^4 M^{-1} s^{-1} [c]	Rate adjusted to give a resting bias of 0.70 for an unstimulated wild-type bacterium.
TWA-Ni^{2+}-stimulated autophosphorylation of CheA TnWA + A → TnWA + Ap	2×10^5 M^{-1} s^{-1} [c]	Adjusted to give a threshold for Ni^{++} for 2×10^{-5} M (Tso and Adler, 1974).
TWA-aspartate-stimulated dephosphorylation of CheY TaWA + Yp → TaWA + Y	1×10^8 M^{-1} s^{-1}	Hypothetical reaction added in order to increase chemotactic gain.
Phosphotransfer from CheAp to CheY Ap + Y → A + Yp	2×10^5 M^{-1} s^{-1}	Lukat *et al.* (1991)
Autophosphorylation of CheY Y → Yp	NA[d]	To account for a low level of CW rotation induced by apparently nonphosphorylated CheY (Barak and Eisenbach, 1992), *bct 1.1* places a lower bound (currently 0.01%) on the fraction of CheY present as CheYp. This may represent autophosphorylation by acetyl phosphtate (Lukat *et al.*, 1992).
Autodephosphorylation of CheYp Yp → Y	3.7×10^{-2} s^{-1}	Lukat *et al.* (1991)
CheZ-stimulated dephosphorylation of CheYp Yp + Z → Y + Z	5×10^5 M^{-1} s^{-1}	Lukat *et al.* (1991)
Phosphotransfer from CheAp to CheB Ap + B → A + Bp	1×10^6 M^{-1} s^{-1}	Data reported by Lupas and Stock (1989) imply a rate of at least 4×10^5 M^{-1} s^{-1}
Autodephosphorylation of CheBp Bp → B	1 s^{-1}	Estimated from phosphate balance

[a] In each case the rate is that of the forward reaction (left-to-right in the above equations); the reverse reaction (right-to-left) is assumed to be zero.

[b] Note that data reported by Hess *et al.* (1988c) and Lukat *et al.* (1991) imply that a faster rate of about 3×10^{-2} s^{-1} in the absence of membranes.

[c] The program estimates the dependence of CheA autophosphorylation on ATP concentration by multiplying these rate constants by the factor ([ATP])([ATP] + K$_m$)$^{-1}$, where K$_m$ is 3×10^{-4} M (Wylie *et al.*, 1988; Bourret *et al.*, 1991; McNally and Matsumura, 1991).

[d] NA, not applicable.

to published observations of wild-type *E. coli* bacteria (see for example Lapidus *et al.*, 1988).

Responses to step changes in either aspartate or Ni^{2+} at different concentrations are plotted in Figure 7. This graph indicates a "threshold" (5% deviation from base-line) for aspartate in the region of 5×10^{-8} M and ~2 $\times 10^{-5}$ M for Ni^{2+}. Although not apparent in this log-arithmic plot, both curves are in fact hyperbolic rather than sigmoidal and thus show no evidence of a cooperative response. The chemotactic gain of the simulation using the core reactions described above was ~0.009, which may be compared with a value of ~0.6 in the same units reported by Segall *et al.* (1986). Inclusion of a hypothetical phosphatase activity (Table 2) that is stimulated by aspartate binding introduces an increased responsiveness to aspartate and increases the gain in proportion to the rate constant assumed for this reaction. A catalytic rate of 9×10^8 M^{-1} s^{-1} produces a gain close to that described by Segall *et al.* (1986). However, this rate constant is larger than commonly observed for pro-

tein-protein interactions (Northrup and Erickson, 1992). The simulations described in this paper therefore employ a more modest rate (1×10^8 M^{-1} s^{-1}) for the hypothetical phosphatase reaction, which generates a gain of 0.08 and shifts the dose-response curve about 10-fold lower in aspartate concentration (Figure 7).

The rapid response to a 5-s pulse of aspartate, delivered at three different concentrations, is shown in Figure 8A. The rotational bias rises to 90% of the plateau value in ~0.5 s for 0.1 μM aspartate, which is the rise time measured by Block *et al.* (1982) following the ionto-phoretic application of an unknown concentration of L-aspartate to tethered *E. coli* cells. These authors also found that the response latency of a CheZ mutant was prolonged in comparison with wild type, and this was again reproduced by the simulation. A mutant lacking CheZ molecules had a rise time of ~2.5 s for a stimulus of 0.1 μM aspartate (Figure 8B). The response to the addition of aspartate is also slower when the simulation
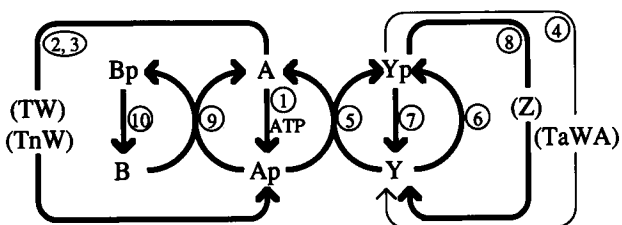
Figure 5. Network of linked protein phosphorylation reactions involved in bacterial chemotaxis. Reactions are numbered as in Table 2. Bold lines indicate reactions demonstrated in vitro. Fine line indicates a hypothetical reaction included in the computer model. Proteins that catalyze reactions without themselves becoming phosphorylated are indicated in parentheses. (TW) and (TnW) represent the catalysis of CheA phosphorylation by CheW and Tar or Tar-Ni^{2+}, respectively, as discussed in the text. (Z) represents the dephosphorylation of CheYp stimulated by CheZ. (TaWA) represents the hypothetical dephosphorylation of CheYp catalyzed by Tar-aspartate, CheW, and CheA.

does not include the hypothetical aspartate-stimulated phosphatase activity (Figure 8B).

Behavioral Mutants

An important feature of this program is the ability to examine the phenotype of any mutant genotype. Any chemotactic component, from Tar to the flagellar motor, can be modified in amount and the consequences for chemotactic performance displayed. The phenotype of a large number of strains of particular interest can be evaluated autonomously.

The performance of selected mutants is listed in Table 5 and compared, where this is known, to the behavior of experimentally observed mutants. Single null mutants lacking each of the proteins Tar, CheW, CheA, CheY, CheZ, or CheB have phenotypes that correspond at least qualitatively to that determined by experiment. Similarly, the model reproduces the phenotype of mutants

in which each of these proteins (except CheA) are individually overexpressed. Table 5 also lists selected mutants in which various combinations of Che proteins are eliminated and/or overexpressed. The phenotype of such mutants, as in the real case, depends on the dosage of the gene in question, but in the majority of cases levels of expression can be found in which the simulated behavior matches that observed experimentally. Of the 47 strains listed in Table 5, 33 have the correct phenotype and 8 have a phenotype at variance with published reports. No experimental data presently exists for the remaining 6 mutant types that are included here as a sample of the very large number of predictions it is possible to make with this program. Any one of the strains listed in Table 5 can be explored in greater detail by examining its response to aspartate or Ni^{2+} or (in the case of overproduction) by changing levels of particular components.

The program was also used to examine the variation in unstimulated swimming behavior produced by systematically changing the levels of selected signaling proteins. Greatest sensitivity was encountered to changes in CheA, and a 10% increase in the concentration of this protein from its wild-type value caused a change in bias of 0.17, or 24%; other proteins in the signal pathway produced smaller changes, in the sequence

CheA > CheZ > CheY > CheB > Tar > CheW

(Table 6). Tests performed over a wider range of concentrations revealed that both CheW and the receptor Tar show a maximal level of tumbling that is diminished at both high and low concentrations (Figure 9).

DISCUSSION

The primary purpose of this model is to summarize and unify existing experimental data into a computer sim-

Table 3. Postulated regulatory interactions between Tar, CheW, and CheA used in the *bct 1.1* simulation

Reaction	k right	k left	Rate constant source/derivation
T + asp ↔ Tasp	1.0×10^6 M^{-1} s^{-1}	1.0 s^{-1}	Average $K_d = 1$ μM for two extreme modification states of Tar (Dunten and Koshland, 1991).
T + ni ↔ Tni	1.0×10^3 M^{-1} s^{-1}	1.0 s^{-1}	K_d unknown. Rate chosen so that response threshold of 2×10^{-5} M (Tso and Adler, 1974) occurs at low receptor occupancy.
T + W ↔ TW	1×10^5 M^{-1} s^{-1} [a]	1.0 s^{-1}	$K_d = 10$ μM (Gegner *et al.*, 1992).
T + A ↔ TA	1×10^4 M^{-1} s^{-1} [a]	1.0 s^{-1}	No direct evidence for this reaction. $K_d \geq 100$ μM (Gegner *et al.*, 1992).
W + A ↔ WA	1×10^5 M^{-1} s^{-1}	1.0 s^{-1}	$K_d = 10$ μM (Gegner and Dahlquist, 1991; Gegner *et al.*, 1992).
TW + A ↔ TWA	4×10^5 M^{-1} s^{-1} [a]	1.0 s^{-1}	$K_d = 3$ μM (Gegner *et al.*, 1992), which implies this rate is about 3×10^5 M^{-1} s^{-1}.
TA + W ↔ TWA	4×10^5 M^{-1} s^{-1} [a]	1.0 s^{-1}	No direct evidence for this reaction. Assumed to have the same rate as Reactions 6 and 8.
T + WA ↔ TWA	4×10^5 M^{-1} s^{-1} [a]	1.0 s^{-1}	$K_d = 2$ μM (Gegner *et al.*, 1992), which implies this rate is about 5×10^5 M^{-1} s^{-1}.

[a] Ligands have no effect on formation of the Tar-CheW-CheA complex (Gegner *et al.*, 1992); therefore in each case the same rate is assumed to apply to the analogous reaction involving Tar or Tar-containing complexes associated with aspartate or Ni^{2+}.

Table 4. "Snapshot" display of signaling species produced by the *bct 1.1* simulation for an unstimulated wild-type bacterium

Signal	Concentration (M)	Signal	Concentration (M)
asp	0.0	Tni-WA	0.0
ni	0.0	A	3.00×10^{-6}
T	3.12×10^{6}	Ap	3.49×10^{-8}
T-asp	0.0	B	1.93×10^{-6}
T-ni	0.0	Bp	6.87×10^{-8}
W	2.89×10^{-6}	Z	2.00×10^{-5}
TW	5.91×10^{-7}	Y	9.99×10^{-6}
Tasp-W	0.0	Yp	7.00×10^{-9}
Tni-W	0.0	M	6.24×10^{-9}
TA	4.44×10^{-7}	MYp	7.77×10^{-10}
Tasp-A	0.0	MYpYp	2.99×10^{-10}
Tni-A	0.0	MYpYpYp	3.78×10^{-10}
WA	6.78×10^{-7}	MYpYpYpYp	2.31×10^{-9}
TWA	8.47×10^{-7}	Bias	0.701[a]
Tasp-WA	0.0		

[a] Bias is a dimensionless quantity, rather than a concentration.

ulation so that it can be easily examined and tested. This has been achieved within a framework that includes a number of hypothetical reaction steps and reaction rates and therefore cannot be correct in every detail. In broad outline, however, the model responds in a correct fashion to a wide range of genetic modifications and stimulus conditions. The rotational bias of the flagellar motor in a range of attractant and repellent concentrations, and the rapidity of the changes in rotation following a sudden change in concentration of aspartate or Ni^{2+} ions, are accurately reproduced. The stochastic performance of individual motors, the durations of runs, tumbles, and pauses they show under various conditions, and the performance of 33 mutants in which individual chemotaxis components have been removed and/or expressed at higher than normal levels, are very similar in the computer-based and the living bacteria.

Limitations exist to the current computer model of the excitation pathway, and we offer several examples that we plan to address in future versions. 1) For the sake of simplicity, the *bct 1.1* simulation allows CheA autophosphorylation to occur only in the free species. Thus the modeled TWA complex does not itself autophosphorylate, but rather stimulates autophosphorylation of free CheA in trans. Another consequence of this programming choice is to account for the phenotype of cells expressing imbalanced levels of various proteins by sequestering CheA in inactive complexes with Tar or CheW. In contrast, there is experimental evidence that CheA autophosphorylation actually does occur within a CheA-CheW complex (McNally and Matsumura, 1991). 2) Both Tar (Milligan and Koshland, 1988) and CheA (Gegner and Dahlquist, 1991) appear to exist predominantly as dimeric species although the model

assumes that they act as monomers. We expect that including the multimeric states of Tar, CheW, and CheA in the model will more accurately reproduce the interactions of these proteins (Swanson *et al.*, 1993). 3) The model also fails to predict correctly the phenotype of a minority of mutant strains examined, notably those containing overproduced CheA (Table 5).

One of the difficulties in developing this simulation was to reproduce the astonishingly large amplification, or gain, of the chemotactic system. Experiments performed by Segall *et al.* (1986) indicate that an increase in receptor occupancy of 1/600 causes a change in rotational bias of about 0.1. It was striking to us that all the approaches we tried using known reactions either failed to give gains of anything like the desired magnitude, or did so in an incomplete, nonphysiological way. Our attempts included a simple displacement scheme in which aspartate competes with CheW for binding to Tar; coupled allosteric interactions between receptor, CheW and other Che proteins; "zero-order
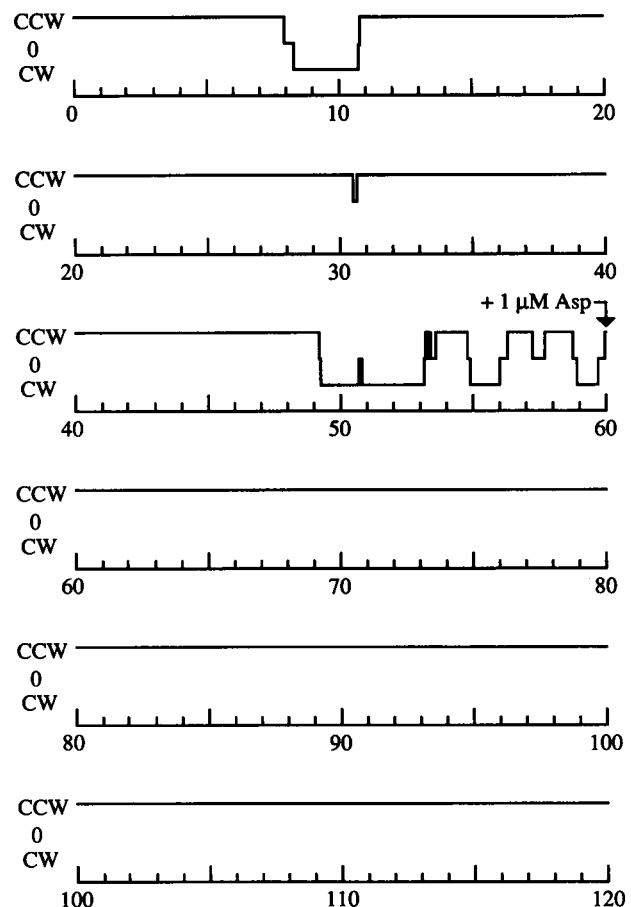

Figure 6. Predicted response of a single flagellar motor to the addition of aspartate. Rotational motion is displayed as CCW (run), 0 (pause), or CW (tumble) for a period of 60 s before and 60 s after the addition of 1 μM aspartate as indicated. Results may be compared with those obtained by Lapidus *et al.* (1988).
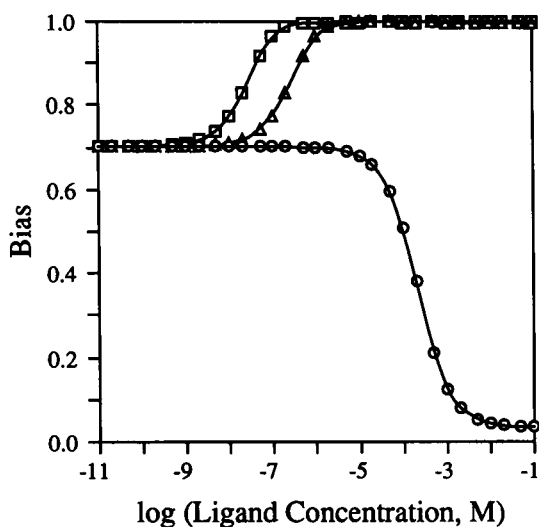
Figure 7. Dose response curves for aspartate (□) and Ni^{2+} (○) in the model. The response to aspartate is also shown for a version of the model lacking the hypothetical TaWA phosphatase activity (△). Each data point was generated by 2000 cycles of simulation after an instantaneous rise in attractant or repellent concentration from 0 to the indicated value.

hypersensitivity" (Koshland, 1987); and a cycle of chemical reactions analogous to the rhodopsin-transducin cycle in the visual system (see Stock *et al.*, 1985).

One parameter we did not introduce is adaptation, which has been deliberately omitted from this model. It may be relevant that in the experiments of Segall *et al.* (1986), mutants lacking CheR and CheB were less sensitive to aspartate than wild-type bacteria by a factor of 10–100—so that from this standpoint the model is correct! We expect that this problem will become resolved in future models that incorporate the methylation reactions of these two proteins.

Thus it appears that the adaptation response may account for a large fraction of the observed amplification in the system. The model helps us examine the question of whether varying the parameters of the excitation process itself could also amplify the signal. Chemotaxis is one example of a large family of environmentally responsive signal transduction networks in prokaryotes (Stock *et al.*, 1989; Bourret *et al.*, 1991). In the nitrogen assimilation and osmolarity systems, the kinases analogous to CheA are known to be involved in dephosphorylation of their CheB/CheY-like substrates (Ninfa and Magasanik, 1986; Keener and Kustu, 1988; Aiba *et al.*, 1989a,b; Igo *et al.*, 1989). As an experiment, we therefore incorporated a hypothetical reaction in which aspartate-liganded TWA complex acts as a phosphatase to remove the phosphoryl group from CheYp. This has the effect of sending a "smooth" signal from a TWA complex bound to aspartate which competes with the tumble signal from unoccupied receptor molecules (carried by TWA in this simulation). Evidence for an inhib-

itory signal transmitted from ligand-occupied receptor has been obtained experimentally (Borkovich and Simon, 1990). The resulting "push-pull" control over CheYp levels, and consequently over motor rotational state, permits relatively large amplifications to be obtained. In the present simulation the gain recorded by (Segall *et al.*, 1986) could be achieved by a reaction rate of 9×10^8 M^{-1} s^{-1} for the CheYp dephosphorylation. Of course, the reaction rate need not be so rapid, because gain probably also comes from adaptation, which is not
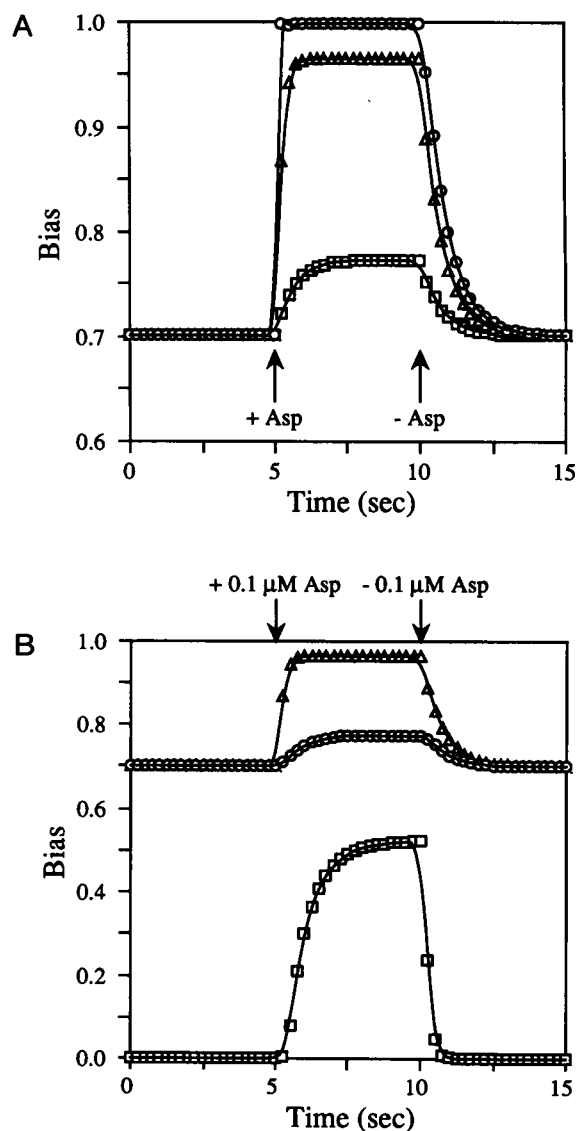

Figure 8. (A) Modeled response of wild-type bacteria to a square-wave pulse of aspartate at 0.01 μM (□), 0.1 μM (△) or 1 μM (○). (B) Modeled response of wild-type bacteria (△), wild-type bacteria lacking the hypothetical TaWA phosphatase activity (○), or mutant bacteria lacking CheZ (□) to a square wave pulse of 0.1 μM aspartate. In each case, aspartate was added at 5 s and removed at 10 s. Note the difference in bias scales between the 2 graphs.

Table 5. Comparison of simulated and observed chemotactic behavior of mutant bacteria

Genotype	Bias Simulated	Bias Observed	Interpretation in terms of *bct 1.1* model	References
Single null mutants				
T[−][b]	sm	sm	Most Yp made by TW-stimulated A	Liu and Parkinson (1989)
B[−]	tm	tm	More p flows to Y in absence of B	Parkinson (1978)
W[−]	sm	sm	Most Yp made by TW-stimulated Y	Parkinson (1978)
A[−]	sm	sm	No Yp	Parkinson (1978)
Y[−]	sm	sm	No Yp	Parkinson (1978)
Z[−]	tm	tm	Yp increases in absence of Z	Parkinson (1978)
Multiple null mutants				
T[−]Z[−]	wt	wt	Unstimulated A makes enough Yp in absence of Z	Liu and Parkinson (1989)
B[−]Z[−]	tm	?	More p flows to Y in absence of B and Z	
T[−]B[−]Z[−]	tm	?	More p flows to Y in absence of B and Z	
W[−]Z[−]	wt	wt	Unstimulated A makes enough Yp in absence of Z	Liu and Parkinson (1989)
T[−]W[−]Z[−]	wt	wt	Unstimulated A makes enough Yp in absence of Z	Liu and Parkinson (1989)
A[−]Z[−]	sm	sm	No Yp, even in absence of Z	Liu and Parkinson (1989)
Y[−]Z[−]	sm	sm	No Yp	Liu and Parkinson (1989)
B[−]Y[−]Z[−]	sm	sm	No Yp	Wolfe et al. (1987)
Overproduction mutants				
T[2+][b]	sm[c]	sm	T overproduction sequesters A and TA complex	Liu and Parkinson (1989)
B[2+]	sm	sm	B removes phosphate from A, thus reducing Yp	Stewart et al. (1988)
W[2+]	sm	sm	W overproduction sequesters A in AW complex	Liu and Parkinson (1989), Sanders et al. (1989)
A[2+]	**tm**[d]	sm	A overproduction leads to more Yp	Stewart et al. (1988)
Y[2+]	tm	tm	Y overproduction leads to more Yp	Clegg and Koshland (1984)
Z[2+]	sm	sm	Z stimulates loss of Yp	Kuo and Koshland (1987)
T[2+]W[2+]	wt[c]	wt	T & W form a complex to restore balance	Liu and Parkinson (1989)
W[2+]A[2+]	**tm**	sm	W overproduction doesn't turn off enough A	Liu and Parkinson (1989), This work
T[2+]A[2+]	tm	?	A overproduction leads to more Yp	
Y[2+]Z[2+]	wt[c]	wt	Z overproduction balances Y overproduction	This work
B[2+]Y[2+]	sm[c]	sm	p flows preferentially through B rather than Y	Stewart et al. (1988)
"Gutted" mutants[a]				
(gutted)	sm	sm	No Yp	Wolfe et al. (1988)
A[+] (gutted)	sm	?	No Yp	
Y[+] (gutted)	sm	sm	No Yp, even in absence of Z	Wolfe et al. (1988)
Y[2+] (gutted)	sm[c]	sm	No YP when Y moderately overproduced	Wolfe et al. (1988)
Y[3+] (gutted)	tm	tm	Very high levels of CheY cause CW rotation	Barak and Eisenbach (1992)
W[+]Y[+] (gutted)	sm	sm	No Yp, even in absence of Z	Conley et al. (1989)
T[+]W[+]Y[+] (gutted)	sm	sm	No Yp, even in absence of Z	Conley et al. (1989)
A[+]Y[+] (gutted)	**tm**	sm	Unstimulated A makes too much Yp in absence of Z	Conley et al. (1989)
A[2+]Y[+] (gutted)	tm	?	A overproduction leads to more Yp	
W[+]A[+]Y[+] (gutted)	**tm**	sm	Unstimulated A makes too much Yp in absence of Z	Conley et al. (1989)
T[+]A[+]Y[+] (gutted)	**tm**	sm	Unstimulated A makes too much Yp in absence of Z	Conley et al. (1989)
T[+]W[+]A[+]Y[+] (gutted)	tm	tm	Stimulated A makes Yp	Conley et al. (1989)
Mixed overproduction/ null mutants				
T[2+]Z[−]	**tm**	wt	T overproduction doesn't turn off enough A	Liu and Parkinson (1989)
B[2+]Z[−]	**tm**	sm	B overproduction doesn't remove enough p from A	This work
W[2+]Z[−]	**tm**	sm	W overproduction doesn't turn off enough A	Liu and Parkinson (1989), Sanders et al. (1989)
A[2+]Z[−]	tm	tm	A overproduction and absence of Z lead to more Yp	This work
Y[2+]Z[−]	tm	?	Y overproduction and absence of Z lead to more Yp	
Y[2+]B[−]Z[−]	tm	tm	More p flows to Y in absence of B and Z	Wolfe et al. (1987)
T[2+]W[−]Z[−]	sm[c]	sm	T overproduction turns off unstimulated A	Liu and Parkinson (1989)
W[2+]B[−]	sm	sm	W overproduction sequesters A, converting B[−] to sm	Sanders et al. (1989)
Z[2+]B[−]	sm	sm	Z overproduction reduces Yp, converting B[−] to sm	Kuo and Koshland (1987)
Y[2+]T[−]	tm	tm	Unstimulated A makes Yp when Y overproduced	Clegg and Koshland (1984)

[a] "Y[+] (gutted)" refers to a strain in which CheY is expressed at wild-type concentration in the absence of Tar or other Che proteins. Swimming behavior predicted by the simulation is characterized as tm = tumble (bias < 0.6), wt = wild type (bias 0.6–0.8), or sm = smooth (bias > 0.8).

[b] The *bct 1.1* model contains only one transducer (Tar), whereas *E. coli* actually has four transducer species. Thus, the behavior of modeled T[−] bacteria are compared with cells lacking all transducers, rather than to a tar single mutant. Furthermore, the available data dictates that modeled cells overexpressing transducer (T[2+]) are compared in this Table with real bacteria that happen to overexpress the Tsr transducer rather than Tar.

[c] "2+" signifies expression at 10X wild-type concentration in the simulation, except in the following cases: T[2+] (13 × T); T[2+]W[2+] (4 × T, 4 × W); Y[2+]Z[2+] (8 × Y, 10 × Z); B[2+]Y[2+] (10 × B, 6 × Y); Y[2+] (gutted) (5 × Y); T[2+]W[−]Z[−] (13 × T).

[d] **underline/bold** entries indicate discrepencies between the model and experiment.

Table 6. Sensitivity of bct 1.1 response to a 10% increase in signaling protein concentration[a]

Signal protein	Change in bias		Change in [CheYp]	
	bias	%	nM	%
Tar	−0.0377	−5.4	+0.285	+4.1
CheB	+0.0430	+6.1	−0.334	−4.8
CheW	−0.0178	−2.5	+0.135	+1.9
CheA	−0.170	−24	+1.31	+19
CheY	−0.0434	−6.2	+0.328	+4.7
CheZ	+0.0796	+11	−0.633	−9.0

[a] Changes in rotational bias and steady state CheYp concentration caused by a 10% increase in the concentration of selected signaling proteins in an otherwise wild-type genetic background (bias = 0.701; [CheYp] = 7.00 nM).

included in the current version of the model. Hypothetical reactions in which CheZ activity is stimulated by Tar-aspartate (or complexes containing Taraspartate) would also enhance gain. Experiments are currently underway to test this prediction. Receptor occupancy has so far been shown experimentally to influence the level of CheY phosphorylation only by regulating the CheA autophosphorylation rate. By highlighting the effect of hypothetical reactions the computer simulation can be a useful tool to motivate and direct experimental work.

Predictions of the Model

The program described in this paper has the capacity to generate an enormous number of experimental predictions. Changes in concentration of signaling molecules in bacteria subjected to a variety of stimuli can be generated at the touch of a key, and this can be done for each of a large number of mutant genotypes, autonomously if required. If we restrict ourselves to situations in which repellent and attractants are each either present (say at 1 mM concentration) or absent, and in which each of six Che proteins can be absent, present in wild-type concentrations, or over-expressed by a factor of 10, then we have 2916 (36 × 4) situations, the majority of which have never been examined experimentally. Since, moreover, the program generates time-courses as well as steady-state levels, so that the response in time of each of more than 20 distinct signaling species can be elaborated for each of the above 2916 situations, its predictive capacity is extremely large.

Most of these predictions, it should be said, are of an "interpolative" nature. Any mutant lacking CheY, for example, may be safely expected to be nonchemotactic and to have a smooth phenotype (although logically speaking, confirmation of even this expectation would add weight to the current model). However there are also numerous genotypes for which the phenotype is not obvious, as illustrated in Table 5.

The simulation also make it possible to predict the sensitivity of the resulting behavior to small variations in the cytoplasmic concentrations of different Che proteins (something that would be extremely difficult to assess experimentally). The present simulation predicts the greatest sensitivity to changes in CheA levels (Table 6, Figure 9), so that a 10% increase of this protein above wild-type levels produces a decrease in rotational bias of 0.17, which is a detectable change in swimming behavior. Levels of synthesis of specific proteins may vary from cell to cell by more than this amount and it will be interesting to see if the introduction of adaptation serves to "damp" these fluctuations and produce a more stable system.

Conclusions

It would be impossible for any contemporary model of bacterial chemotaxis to be correct in every respect. Many of the rate constants and virtually all of the intracellular signaling concentrations on which such a model would depend are unknown. Even the biochemical "circuitry" itself has not been fully agreed upon. We know that a cascade of protein phosphorylation reactions carries information from the receptors to the flagellar motors, but further details, such as precisely how Tar, CheW, and CheA interact, remain a matter of conjecture.

Despite this uncertainty, the results presented in this paper demonstrate that the model we have tested, which is based on a compilation of widely accepted mechanisms, provides an adequate explanation for most of the short-term chemotactic responses. The computer simulation has allowed us to apply a very large number
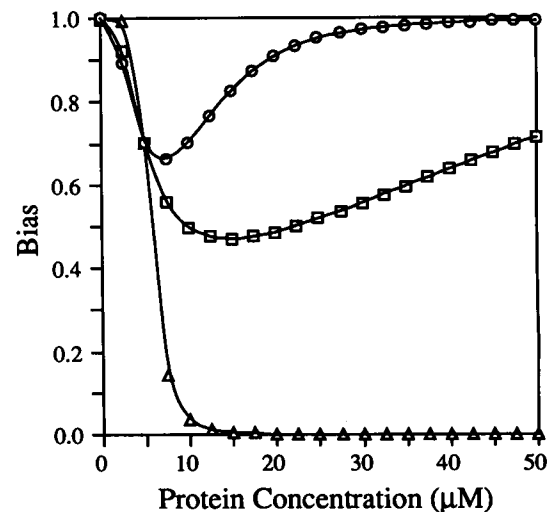

Figure 9. Modeled changes in rotational bias of unstimulated mutant bacteria expressing different levels of the Tar (□), CheW (○), or CheA (△) proteins. The intracellular concentration of each protein in a wild-type bacterium is 5 μM. Each data point was generated by 2000 cycles of simulation.

of tests "at one sitting" in a way that would be hardly feasible in the real world. We have been able to modify the biochemical characteristics and genetic background of simulated bacteria and evaluate their behavioral consequences instantly, comparing them with relevant published experimental data, where this exists. Although modifications to the program will become necessary as it is extended to include the methylation reactions associated with adaptation and as new experimental data becomes available, the underlying framework should be sufficiently robust to accommodate these changes.

ACKNOWLEDGMENTS

REFERENCES

Aiba, H., Mizuno, T., and Mizushima, S. (1989a). Transfer of phosphoryl group between two regulatory proteins involved in osmoregulatory expression of the ompF and ompC genes in Escherichia coli. J. Biol. Chem. 264, 8563–8567.

Aiba, H., Nakasai, F., Mizushima, S., and Mizuno, T. (1989b). Evidence for the physiological importance of the phosphotransfer between the two regulatory components, EnvZ and OmpR, in osmoregulation in Escherichia coli. J. Biol. Chem. 264, 14090–14094.

Asakura, S., and Honda, H. (1984). Two-state model for bacterial chemoreceptor proteins. The role of multiple methylation. J. Mol. Biol. 176, 349–367.

Barak, R., and Eisenbach, M. (1992). Correlation between phosphorylation of the chemotaxis protein CheY and its activity at the flagellar motor. Biochemistry 31, 1821–1826.

Berg, H.C., and Brown, D.A. (1972). Chemotaxis in Escherichia coli analysed by three-dimensional tracking. Nature 239, 500–504.

Block, S.M., Segall, J.E., and Berg, H.C. (1982). Impulse responses in bacterial chemotaxis. Cell 31, 215–226.

Block, S.M., Segall, J.E., and Berg, H.C. (1983). Adaptation kinetics in bacterial chemotaxis. J. Bacteriol. 154, 312–323.

Borkovich, K.A., Alex, L.A., and Simon, M.I. (1992). Attenuation of sensory receptor signaling by covalent modification. Proc. Natl. Acad. Sci. USA 89, 6756–6760.

Borkovich, K.A., Kaplan, N., Hess, J.F., and Simon, M.I. (1989). Transmembrane signal transduction in bacterial chemotaxis involves ligand-dependent activation of phosphate group transfer. Proc. Natl. Acad. Sci. USA 86, 1208–1212.

Borkovich, K.A., and Simon, M.I. (1990). The dynamics of protein phosphorylation in bacterial chemotaxis. Cell 63, 1339–1348.

Bourret, R.B., Borkovich, K.A., and Simon, M.I. (1991). Signal transduction pathways involving protein phosphorylation in prokaryotes. Annu. Rev. Biochem. 60, 401–441.

Bourret, R.B., Davagnino, J., and Simon, M.I. (1993). The carboxy-terminal portion of the CheA kinase mediates regulation of autophosphorylation by transducer and CheW. J. Bacteriol. 175, (in press).

Bourret, R.B., Hess, J.F., and Simon, M.I. (1990). Conserved aspartate residues and phosphorylation in signal transduction by the chemotaxis protein CheY. Proc. Natl. Acad. Sci. USA 87, 41–45.

Clarke, S., and Koshland, D.E., Jr. (1979). Membrane receptors for aspartate and serine in bacterial chemotaxis. J. Biol. Chem. 254, 9695–9702.

Clegg, D.O., and Koshland, D.E., Jr. (1984). The role of a signaling protein in bacterial sensing: behavioral effects of increased gene expression. Proc. Natl. Acad. Sci. USA 81, 5056–5060.

Conley, M.P., Wolfe, A.J., Blair, D.F., and Berg, H.C. (1989). Both CheA and CheW are required for reconstitution of chemotactic signaling in Escherichia coli. J. Bacteriol. 171, 5190–5193.

DeFranco, A.L., and Koshland, D.E., Jr. (1981). Molecular cloning of chemotaxis genes and overproduction of gene products in the bacterial sensing system. J. Bacteriol. 147, 390–400.

Dunten, P., and Koshland, D.E., Jr. (1991). Tuning the responsiveness of a sensory receptor via covalent modification. J. Biol. Chem. 266, 1491–1496.

Dupont, G., and Goldbeter, A. (1992). Oscillations and waves of cytosolic calcium: insights from theoretical models. Bioessays 14, 485–493.

Eisenbach, M., Wolf, A., Welch, M., Caplan, S.R., Lapidus, I.R., Macnab, R.M., Aloni, H., and Asher, O. (1990). Pausing, switching and speed fluctuation of the bacterial flagellar motor and their relation to motility and chemotaxis. J. Mol. Biol. 211, 551–563.

Fersht, A. (1984). Enzyme Structure and Mechanism, 2nd ed., San Francisco, CA: W.H. Freeman.

Gegner, J.A., and Dahlquist, F.W. (1991). Signal transduction in bacteria: CheW forms a reversible complex with the protein kinase CheA. Proc. Natl. Acad. Sci. USA 88, 750–754.

Gegner, J.A., Graham, D.R., Roth, A.F., and Dahlquist, F.W. (1992). Assembly of an MCP receptor, CheW and kinase CheA complex in the bacterial chemotaxis signal transduction pathway. Cell 70, 975–982.

Goldbeter, A., and Koshland, D.E., Jr. (1982). Simple molecular model for sensing and adaptation based on receptor modification with application to bacterial chemotaxis. J. Mol. Biol. 161, 395–416.

Hazelbauer, G.L., and Engstrom, P. (1981). Multiple forms of methyl-accepting chemotaxis proteins distinguished by a factor in addition to multiple methylation. J. Bacteriol. 145, 35–42.

Hess, J.F., Bourret, R.B., Oosawa, K., Matsumura, P., and Simon, M.I. (1988a). Protein phosphorylation and bacterial chemotaxis. Cold Spring Harbor Symp. Quant. Biol. 53, 41–48.

Hess, J.F., Bourret, R.B., and Simon, M.I. (1988b). Histidine phosphorylation and phosphoryl group transfer in bacterial chemotaxis. Nature 336, 139–143.

Hess, J.F., Oosawa, K., Kaplan, N., and Simon, M.I. (1988c). Phosphorylation of three proteins in the signaling pathway of bacterial chemotaxis. Cell 53, 79–87.

Igo, M.M., Ninfa, A.J., Stock, J.B., and Silhavy, T.J. (1989). Phosphorylation and dephosphorylation of a bacterial transcriptional activator by a transmembrane receptor. Genes Dev. 3, 1725–1734.

Jones, C.J., and Aizawa, S.-I. (1991). The bacterial flagellum and flagellar motor: structure, assembly and function. Adv. Microb. Physiol. 32, 109–172.

Keener, J., and Kustu, S. (1988). Protein kinase and phosphoprotein phosphatase activities of nitrogen regulatory proteins NtrB and NtrC of enteric bacteria: roles of the conserved amino terminal domain of NtrC. Proc. Natl. Acad. Sci. USA 85, 4976–4980.

Koshland, D.E., Jr. (1987). Switches, thresholds, and ultrasensitivity. Trends Biochem. Science 12, 225–229.

Kuo, S.C., and Koshland, D.E., Jr. (1987). Roles of *cheY* and *cheZ* gene products in controlling flagellar rotation in bacterial chemotaxis of *Escherichia coli*. J. Bacteriol. *169*, 1307–1314.

Kuo, S.C., and Koshland, D.E., Jr. (1989). Multiple kinetic states for the flagellar motor switch. J. Bacteriol. *171*, 6279–6287.

Lamb, T.D., and Pugh, E.N. (1992). A quantitative account of the activation steps involved in phototransduction in amphibian photoreceptors. J. Physiol. *449*, 719–758.

Lapidus, I.R., Welch, M., and Eisenbach, M. (1988). Pausing of flagellar rotation is a component of bacterial motility and chemotaxis. J. Bacteriol. *170*, 3627–3632.

Larsen, S.H., Reader, R.W., Kort, E.N., Tso, W.-W., and Adler, J. (1974). Change in direction of flagellar rotation is the basis of the chemotactic response in *Escherichia coli*. Nature *249*, 74–77.

Liu, J., and Parkinson, J.S. (1989). Role of CheW protein in coupling membrane receptors to the intracellular signaling system of bacterial chemotaxis. Proc. Natl. Acad. Sci. USA *86*, 8703–8707.

Lukat, G.S., Lee, B.H., Mottonen, J.M., Stock, A.M., and Stock, J.B. (1991). Roles of the highly conserved aspartate and lysine residues in the response regulator of bacterial chemotaxis. J. Biol. Chem. *266*, 8348–8354.

Lukat, G.S., McCleary, W.R., Stock, A.M., and Stock, J.B. (1992). Phosphorylation of bacterial response regulator proteins by low molecular weight phospho-donors. Proc. Natl. Acad. Sci. USA *89*, 718–722.

Lupas, A., and Stock, J. (1989). Phosphorylation of an N-terminal regulatory domain activates the CheB methylesterase in bacterial chemotaxis. J. Biol. Chem. *264*, 17337–17342.

Matsumura, P., Roman, S., Volz, K., and McNally, D. (1990). Signalling complexes in bacterial chemotaxis. In: Biology of the Chemotactic Response, ed. J.P. Armitage and J.M. Lackie, Cambridge, UK: Cambridge University Press, 135–154.

McNally, D.F., and Matsumura, P. (1991). Bacterial chemotaxis signaling complexes: formation of a CheA/CheW complex enhances autophosphorylation and affinity for CheY. Proc. Natl. Acad. Sci. USA *88*, 6269–6273.

Michaelis, M., und Menten, M.L. (1913). Die Kinetik der Invertinwirkung Biochem Z *49*, 333–369.

Milligan, D.L., and Koshland, D.E., Jr. (1988). Site directed crosslinking establishing the dimeric structure of the aspratate receptor of bacterial chemotaxis. J. Biol. Chem. *263*, 6268–6275.

Ninfa, A.J., and Magasanik, B. (1986). Covalent modification of the *glnG* product, NR₁, by the *glnL* product, NR₁₁, regulates transcription of the *glnALG* operon in *Escherichia coli*. Proc. Natl. Acad. Sci. USA *83*, 5909–5913.

Ninfa, E.G., Stock, A., Mowbray, S., and Stock, J. (1991). Reconstitution of the bacterial chemotaxis signal transduction system from purified components. J. Biol. Chem. *266*, 9764–9770.

Northrup, S.H., and Erickson, H.P. (1992) Kinetics of protein-protein association explained by Brownian dynamics computer simulation. Proc. Natl. Acad. Sci. USA *89*, 3338–3342.

Parkinson, J.S. (1978). Complementation analysis and deletion mapping of *Escherichia coli* mutants defective in chemotaxis. J. Bacteriol. *135*, 45–53.

Sanders, D.A., Mendez, B., and Koshland, D.E., Jr. (1989). Role of the CheW protein in bacterial chemotaxis: overexpression is equivalent to absence. J. Bacteriol. *171*, 6271–6278.

Segall, J.E., Block, S.M., and Berg, H.C. (1986). Temporal comparisons in bacterial chemotaxis. Proc. Natl. Acad. Sci. USA *83*, 8987–8991.

Segall, J.E., Ishihara, A., and Berg, H.C. (1985). Chemotactic signaling in filamentous cells of *Escherichia coli*. J. Bacteriol. *161*, 51–59.

Segall, J.E., Manson, M.D., and Berg, H.C. (1982). Signal processing times in bacterial chemotaxis. Nature *296*, 855–857.

Segel, I.H. (1975). Enzyme Kinetics: Behavior and Analysis of Rapid Equilibrium and Steady State Enzyme Systems. New York: John Wiley & Sons.

Silverman, M., and Simon, M. (1974). Flagellar rotation and the mechanism of bacterial motility. Nature *249*, 73–74.

Springer, W.R., and Koshland, D.E., Jr. (1977). Identification of a protein methyltransferase as the *cheR* gene product in the bacterial sensing system. Proc. Natl. Acad. Sci. USA *74*, 533–537.

Stewart, R.C., Roth, A.F., and Dahlquist, F.W. (1990). Mutations that affect control of the methylesterase activity of CheB, a component of the chemotaxis adaptation system in *Escherichia coli*. J. Bacteriol. *172*, 3388–3399.

Stewart, R.C., Russell, C.B., Roth, A.F., and Dahlquist, F.W. (1988). Interaction of CheB with chemotaxis signal transduction components in *Escherichia coli*: modulation of the methylesterase activity and effects on cell swimming behavior. Cold Spring Harbor Symp. Quant. Biol. *53*, 27–40.

Stock, A., Koshland, D.E., Jr., and Stock, J. (1985). Homologies between the *Salmonella typhimurium* CheY protein and proteins involved in the regulation of chemotaxis, membrane protein synthesis, and sporulation. Proc. Natl. Acad. Sci. USA *82*, 7989–7993.

Stock, J.B., Kersulis, G., and Koshland, D.E., Jr. (1985). Neither methylating nor demethylating enzymes are required for bacterial chemotaxis. Cell *42*, 683–690.

Stock, J.B., and Koshland, D.E., Jr. (1978). A protein methylesterase involved in bacterial sensing. Proc. Natl. Acad. Sci. USA *75*, 3659–3663.

Stock, J.B., Lukat, G.S., and Stock, A.M. (1991). Bacterial chemotaxis and the molecular logic of intracellular signal transduction networks. Annu. Rev. Biophys. Biophys. Chem. *20*, 109–136.

Stock, J.B., Ninfa, A.J., and Stock, A.M. (1989). Protein phosphorylation and regulation of adaptive responses in bacteria. Microbiol. Rev. *53*, 450–490.

Stock, J.B., Surette, M.G., McCleary, W.R., and Stock, A.M. (1992). Signal transduction in bacterial chemotaxis. J. Biol. Chem. *267*, 19753–19756.

Swanson, R.V., Bourret, R.B., and Simon, M.I. (1993). Intermolecular complementation of the kinase activity of CheA. Mol. Microbiol. *7*, (*in press*).

Tso, W.-W., and Adler, J. (1974). Negative chemotaxis in *Escherichia coli*. J. Bacteriol. *118*, 560–576.

Wolfe, A.J., Conley, M.P., and Berg, H.C. (1988). Acetyladenylate plays a role in controlling the direction of flagellar rotation. Proc. Natl. Acad. Sci. USA *85*, 6711–6715.

Wolfe, A.J., Conley, M.P., Kramer, T.J., and Berg, H.C. (1987). Reconstitution of signaling in bacterial chemotaxis. J. Bacteriol. *169*, 1878–1885.

Wylie, D., Stock, A., Wong, C.-Y., and Stock, J. (1988). Sensory transduction in bacterial chemotaxis involves phosphotransfer between Che proteins. Biochem. Biophys. Res. Commun. *151*, 891–896.